New method for statistical analysis of climate time series

Eric Zeltz

ACCSCIENCE PUBLISHING

Explora: Environment and Resource

ORIGINAL RESEARCH ARTICLE

New method for statistical analysis of climate time series

Eric Zeltz*

Independent Scholar, La Motte en Champsaur, Hautes-Alpes, France

Abstract

After publishing four articles utilizing a new method for the statistical study of climate time series, we found it useful to provide a detailed review of the method itself, which is the primary objective of this work. Unlike the methods most commonly used by scientists analyzing such data, this new method does not seek to identify trends for explorative forecasts. Instead, it enables the detection of precise signals indicating interactions with other climate entities, thereby enhancing our understanding of the underlying phenomena. As illustrated through three example articles, the mechanisms uncovered using this method can be integrated into a mathematical model. The simulations thus obtained are more deterministic than stochastic – a significant advantage for producing high-quality forecasts in the context of global warming. Even if this was the sole application of the method, it would be sufficient to demonstrate its value. However, as a final example detailed in this work shows, reconsidering the original series using different periods (e.g., month, quarter, semester, year) can further refine our understanding of the mechanisms at play. We conclude this work by exploring the potential applicability of this method for analyzing non-climatic temporal data series.

Keywords: Climate time series; Markov chains; Signals; Statistical analysis method

***Corresponding author:**
Eric Zeltz
(ericzeltz@wanadoo.fr)

Citation: Zeltz E. New method for statistical analysis of climate time series. *Explora Environ Resour.* doi: 10.36922/eer.6109

Received: November 17, 2024

1st revised: December 21, 2024

2nd revised: January 14, 2025

Accepted: January 16, 2025

Published Online: February 6, 2025

1. Introduction

Time series theory[1] has enabled great advances in sciences as well as in econometrics, information theory, demography, and astronomy.[2-5]

The application of this theory facilitates the isolation of trends as well as the identification of value stability and variations within the analyzed series. Based on this approach, it is possible to generate robust future or past projections, which often demonstrate greater reliability compared to those derived from even highly sophisticated structural models.

A major challenge in climatology is to obtain, from data collected in the form of time series, projections on the future of the parameters in question, accompanied by error bars, without which these projections would not be of real use.[6]

The classic approach begins with a climate equation that projects the climatic variable X(t) at time step t as the sum of a "trend" component $X_{trend}(t)$ and a "noise" component $X_{noise}(t)$, which reflects, for example, natural variability.

Often the equation is in this simple form: $X(t) = X_{trend}(t) + S(t) X_{noise}(t)$.

The main difficulty lies in obtaining a reliable estimate for the X_{trend} statistical trend from the known time series. Estimation methods are well developed and include linear curves (e.g., classic linear regression),[7,8] which may incorporate breaks,[9] accelerated increases or decreases,[10,11] along with "bootstrap" confidence intervals.[12,13] These methods also extend to non-linear behaviors or even non-parametric descriptions.[14-16] Mudelsee[6] gives a fairly complete overview of these methods, which are numerous and more or less complex, aiming to extract estimates from the data, accompanied by measures of uncertainty.

Even though the method presented in this article also starts from the raw data provided by climate time series, the initial approach is not the same. It does not seek to obtain estimates of future trends from the data but simply looks for possible "signals" of interactions with the time series of other climate entities whose signals are compatible with that of the initial series. These signals are obtained from the average lengths of increasing or decreasing chains of the studied climate parameter. The method is therefore referred to as the method of average lengths, or simply "MAL." Once these signals are detected and the climate mechanisms underlying their interactions are thoroughly explained, they can be incorporated into a climate model. Each instance in which the method isolates new interactions and elucidates their mechanisms contributes to significant improvement in the climate model.

Other methods exist to check the compatibility of time series and investigate the causal relationships. Starting with the calculation of the correlation coefficient between the two series concerned. But as we will see, it is possible that two series do not have a significant correlation and yet signals MAL are in agreement. This therefore indicates that MAL can detect invisible interactions by more classic means. This is also the case with techniques that are nevertheless much more sophisticated than the simple calculation of the correlation coefficient. For example, the use of the concept of co-integration introduced by Granger and Newbold[17] in econometrics facilitates the detection of long-term relationships between two or more time series. Several algorithms can be used to verify this, such as the Granger–Engle algorithm,[18] the Johansen approach,[19] the Stock–Watson test,[20] or the Phillips–Ouliar test.[21] Tests are also available to verify causal relationships and their significance between two digital entities represented by time series, such as the Granger causality test.[22] These methods are often well-suited for analyzing econometric time series in particular. However, in the studied climate series, we observed that traditional methods could be inapplicable or inconclusive in terms of co-integration or causality, despite the presence of MAL signals that showed strong correspondence. In other words, MAL proves to be more efficient and capable of detecting interrelationship signals that remain invisible to classical techniques. These signals, in turn, enable a deeper understanding of the underlying climate mechanisms.

This article is divided into three main parts:

1. Description of MAL: This first part presents the main idea of the MAL and what are the stages of its implementation.
2. Examples of MAL utilization in climatology: Four recent articles on mathematic models applied in climatology (Zeltz[23-26]) employ this new method for the statistical analysis of time series. As will be discussed in subsequent sections, MAL enables the identification of interactions that would likely remain undetected using traditional methods for studying numerical series, such as those presented by Mudelsee.[6] In the four sections of this second part, we show the implementation of MAL and address the questions that arose during its initial applications.[23-26]
3. Evaluation and perspective of MAL: We summarize here the strengths and weaknesses of MAL and provide a detailed example illustrating its utility in understanding the mechanisms at play across different time steps (e.g., months, quarters). Finally, we explore the potential applicability of MAL in fields beyond climatology.

2. Description of MAL

2.1. Sample introduction

Suppose there is a well-balanced coin with an equal probability of 0.5 for landing heads (denoted as H) or tails (denoted as T). If this coin is tossed 100 times, we record each successive outcome. The probability of obtaining a perfectly alternating sequence such as HTHTHT.HTHT is exceedingly small, specifically $(½)^{100}$, or less than one chance in a billion billion billion. This scenario is governed by a binomial law X~B (n = 100, P = 0.5). According to Delmas,[27] the expected distribution of successive heads (and similarly for tails) follows the mathematical expectations shown in Table 1.

In addition, the theoretical average length of the substrings is approximately 1.94.

Table 1. Theoretical frequencies for substrings of heads (H) or tails (T) of a certain length in a series of 100 coin tosses

Length	1	2	3	4	5	6	7 and more
Theoretical frequencies (%)	51	25	12.5	6	3.5	0.9	1.1

Now let's return to our sequence of one hundred throws. The experiment completed, we realize that in fact, the average length of the chains of successive H (or T) is clearly less than the theoretical figure of 1.94, that there are many more chains of 1 and 2 than predicted by the frequencies and much less for channels of 3 and more. The alternation is therefore much faster than predicted by theory. This can happen, and at this point, there is no reason to question the truly binomial character of the experiment.

On the other hand, if we repeat this experience of 100 tosses ten times in a row, and each time we find a clearly accelerated alternation, it becomes necessary to question the underlying cause. It is almost impossible for this to be a result of pure chance, and since the coin is perfectly balanced, the cause is most likely an interaction with an external phenomenon. The precise origin of this interaction – whether a periodic electromagnetic influence or another factor – cannot be determined without further investigation. Nonetheless, we can assert with high confidence that an external interaction is at play. This consistently shorter-than-expected average length of successive H (or T) chains serves as a "signal" indicating such an interaction.

This is the core concept of MAL: if, in a given time series with two equally probable outcomes A or B, the vast majority of chains of 100 successive outcomes exhibit significantly lower average lengths of successive A (orB) subchains at 1.94, it is reasonable to suspect the existence of an interaction with another entity that explains the stronger-than-expected alternation. Conversely, if the average lengths are significantly higher than 1.94, the hypothesis of an interaction must also be seriously considered.

If the time series in question concerns a certain climatic entity with two equally probable outcomes, these average lengths can serve as the "signals" indicating the presence of interactions with other climatic entities. A priori, it will be necessary to identify potential interactions among entities whose numerical data exhibit concordant signals, enabling effective selection for further investigation.

2.2. The main steps of MAL

Consider a certain time series concerning a climatic parameter with numerical values. The following steps outline its processing using MAL:

1. From the initial series, generate a second series consisting of "gaps," defined as the difference between each term in the initial series and the one immediately preceding it.
2. Verify whether this series of gaps can be modeled as "white noise" (p. 45 of Hamilton[1]). "White noise" refers to a series with no trend in either its mean or the standard deviation and with empirically calculated correlations that are nearly zero and independent of their positions in time.
3. Create a third series consisting of 1s and 0s by assigning the value 1 to each gap if it is positive and 0 otherwise. Then, verify that the point frequencies of 0s and 1s are both close to 0.5, ensuring that increases and decreases in the studied parameter can reasonably be considered equiprobable.
4. If either of the previous two steps fails, MAL cannot be used. However, if both conditions are satisfied, all prerequisites are met for modeling the binary series of 1s and 0s using a Markov chain (p. 682 of Hamilton[1]).
5. The temporal spacing (e.g., day, month, quarter, year) used in the initial time series, along with the "climatic memory" of the phenomenon, must be taken into account to determine the appropriate orders for the Markov chains. Based on these two parameters, only orders 0 and 1 were applicable in the four studies.[23-26] The following terminology is used to describe average chain lengths: (A) Close to 1.94: Markov-0 signal; (B) Significantly lower than 1.94: Markov-1 alternating signal; (C) Significantly higher than 1.94: Markov-1 lengthening signal. However, nothing precludes the possibility that higher-order Markov chains may be more adequate, especially when the climatic memory of the phenomenon significantly exceeds the length of the time series.
6. In the event of uncertainty between two possible orders, calculating the probabilities of obtaining the observed chain lengths for each potential order allows for determining which order is most appropriate for modeling the series.
7. In the case of order 0, the MAL does not reveal any signal of interaction with another climatic entity, though this does not mean there is none. However, as soon as the order is ≥1, as seen in the introductory example, it is a strong indication of an interaction with one or more other entities.
8. In this latter case, the next step is to identify these entities and verify that the signals observed in them are consistent with the proposed explanation.
9. The MAL method concludes at this point. It is then the responsibility of climatology and modeling to validate the proposed explanations.

3. Examples of MAL application in climatology

3.1. The first application of MAL

In the first study on MAL,[23] fluctuations in the global monthly average atmospheric temperature were analyzed

over the period 1880 – 2015. The detailed statistical study yielded two key findings:

1. Regardless of the sub-period of 100 consecutive months examined among the sixteen covering the 1880 – 2015 time frame, the frequencies of temperature rise or fall were approximately the same – very close to equiprobability.
2. Taking into account, the average lengths of the chains of ascents or descents – all <1.94 and most of them very clearly on the sixteen chains of 100 months analyzed – it was highly improbable (probability less than 1 in 60,000) that these fluctuations were governed by a binomial distribution with parameters $n = 100$ and $P = 0.5$. The result obtained in a given month (rise or fall) appeared to significantly increase the probability of reversal in the following month (fall or rise). Hence, the author proposed that these fluctuations are better modeled as first-order Markov chains, which he describes as "alternating," since the alternation is faster than what is expected under a binomial model.

All the steps described in Section 2.2 were then carefully verified, allowing the author to conclude that these chains were of Markov-1 alternating type.

MAL, therefore, was already largely developed and finalized in this first article.

The hypothesis put forward to explain this accelerated alternation was the following:

1. "When the atmosphere of the globe warms up, whatever the reason, the evaporation that this causes on the oceans and the land ends up increasing the low cloud cover. This development of low clouds then refreshes the atmosphere through the strong albedo effect of these clouds, as well as through the precipitation they bring.
2. If, on the contrary, the globe's atmosphere cools, there is less evaporation, therefore, fewer low clouds. The overall albedo effect of clouds decreases, which allows solar heat to better penetrate to the surface of the globe (Section IV-2 of the first study[23])

Its validation was based only on very partial cloudiness data (period 1983 – 2005) obtained from slide 10 of Taboada.[28] At the time, the author did not have more complete data on cloud cover and he was aware of the fragility of his conclusions since he added this:

"It is also regrettable that we do not have such a study over a much longer period because this would have made it possible to directly study the correlation between NOAA data and that of low cloud cover." (Section IV-2 of the first study[23]).

3.2. The second applications of MAL

As the previous explanation did not seem sufficient to be entirely conclusive, the author proposed a second explanatory hypothesis in another study.[24] This time, the second variable considered for interaction with the global average atmospheric temperature was the heat received by the Upper Oceanic Stratum (UOS) within the 0 and −700 m depth range.

For this analysis, he used quarterly data on the anomalies of this heat over a period of nearly 70 years (1955 – 2022), a duration long enough for a reliable study of the proposed hypothesis.

After processing the data as outlined in Section 2.2, he observed a distinct Markov-1 alternating behavior, similar to that seen in atmospheric temperature data, though with the key difference that these data were recorded quarterly rather than monthly.

In summary, as detailed in Section 3.1 of this study,[24] the author proposed the following principle of interaction:

The warming of the atmosphere in a given month causes evaporation, which requires calories drawn from the UOS, resulting in its cooling. With a certain inertia of the order of a month, this cooling propagates by conduction or convection into the ambient atmosphere, which increases the probability of atmospheric cooling in the following month. On the contrary, the cooling of the atmosphere in a given month reduces evaporation, meaning fewer calories are drawn from the UOS. As a result, incoming heat, particularly from solar rays, is more readily retained in the UOS, causing it to warm. This heat is then transferred to the surrounding atmosphere, thereby increasing the probability of atmospheric warming in the following month.

The quarterly, rather than monthly, alternation of the UOS heat anomalies is explained by the author in the following way: the thermal inertia of the UOS is significantly greater than that of the atmosphere. As a result, a duration on the order of a quarter is required for atmospheric events to produce visible and measurable repercussions on the heat received by the UOS. However, due to the accelerated monthly alternation of atmospheric conditions – faster than what would be expected under a binomial distribution – there is a higher likelihood that, over the course of a quarter, the monthly atmospheric averages follow one of the two patterns.

- Rise, then fall, then rise, leading to a greater likelihood of positive than negative results for the quarter in question.
- Fall, then rise, then fall, resulting in a greater likelihood of a negative than positive balance for the quarter in question.

To verify the consistency of this proposed explanation with the observations, the author developed a mathematical model (called Z.1) that takes into account the energy exchanges between the sun, the troposphere, and the UOS while integrating the hypothesized interaction between the UOS heat and atmospheric temperature. The constants in the model were calibrated using the data observed during the period 1955 – 2022. The Z.1 program is explained and summarized in Table 7 of the study.[24] We have reproduced Figure 1 of the study[24] as Figure 2 here. The figure presents the observed evolutions of the atmospheric temperature and UOS heat over the period 1955 – 2022, as well as the simulations obtained for these two temperatures over the period 1955 – 2095, generated by the Z.1 model.

Ultimately, the study[24] did not bring anything new for MAL itself compared to the previous study.[23] However, the validation of the explanations for the signals obtained through MAL is notably more thorough, and the simulations obtained using Model Z.1 provide strong support for the consistency of the proposed hypothesis with the observations. Furthermore, these simulations, generated quickly on a simple microcomputer, provide fairly precise information on the medium-term evolution of two of the most important parameters of the Earth's climate.

We can also note that on certain aspects, the method used in the study is reminiscent of Hasselmann's theory.[29] Like our approach, Hasselmann's theory involves Markov chains and takes into account different climatic memories of the world ocean and the atmosphere. It, therefore, seems interesting to precisely compare these two methods.

In Hasselmann's theory, short-term random noise (atmospheric weather) leads to longer-term variations (red spectra at the ocean level). This is mathematically modeled using a first-order autoregressive process, where the next step y_{t+1} of the long-term variation depends on the previous step y_t, weighted by the climatic memory m of the ocean, and is disturbed by short-term variability x_t:

$$y_{t+1} = m\, y_t + x_t$$

In our case, it is the "signals" detected that initially guide us: A Markov-1 alternating-type signal is observed for both atmospheric (monthly) and oceanic (quarterly) temperatures. This suggests the presence of an interaction, and the hypothesis formulated in the Z.1 model posits a direct interaction between the two. The difference in periodicity between the two signals is attributed to the vastly different climatic memories of the atmosphere and the ocean.

The Z.1 model is built on this interaction and has nothing stochastic apart from the fact that we introduced random coefficients to take into account natural variability. Thus, our model is more deterministic and less stochastic compared to Hasselmann's, even though both emphasize the critical role of climate memory in the framework.

3.3. The third application of MAL

In another subsequent study,[25] the author returns to a question that he had already addressed in the first study[23]: the influence of cloudiness on the climate. Having at his disposal oceanic cloud cover data spanning a long period

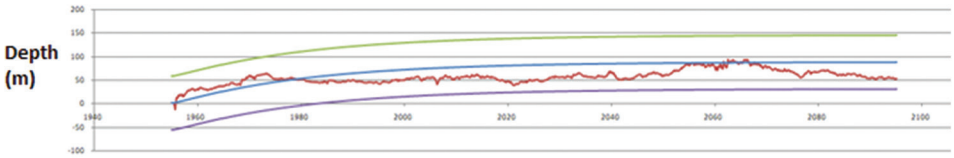

Figure 1. Simulations of Z.3 model for deepening. Reproduced from Zeltz[26]. Notes: Red curve: Simulation of anomalies of deepening, Sn (m). For the other curves: The 95% confidence interval is delimited by the upper curve and lower curve. The central blue curve is the theoretical curve (without taking into account natural variability) of the deepening anomalies.

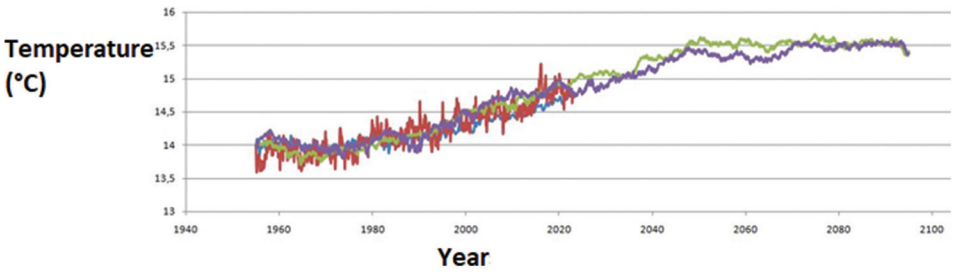

Figure 2. Simulations of t_n and θ_n over the period 1955 – 2095 compared to the observed temperatures of Ta_n and Θ_n during the period 1955 – 2022. Copyright © 2024 Author(s). Reproduced from Zeltz[24]. Notes: Red curve: observed atmospheric temperature, Ta_n; Purple curve: simulated atmospheric temperature, t_n; Blue curve: Observed upper ocean layer temperature, Θ_n; Green curve: simulated upper ocean layer temperature, θ_n.

– much longer than for those used in 2021 – the author applied MAL to the following data series:

- Ocean cloudiness (OC): The series of average quarterly diurnal anomalies for the period 1954 – 2008 obtained from meteorological reports recorded aboard ships and updated according to the standards of the World Meteorological Organization (further details on these data in Eastman *et al.*[30]
- UOS heat: The series of the quarterly average anomalies between 0 and −700 m depth range sourced from a database previously used in the second study[24] (downloadable from the provided link[1]). This dataset starts in 1955, overlapping with the OC database for 216 quarters, covering the period from 1955 to 2009.

Their analysis using MAL shows a clearMarkov-1 alternating signal for both datasets, along with a significant correlation (0.65) between them. This led to a hypothesis of an interaction between the two, which the author explains as follows:

"During a quarter the UOS warms up, this causes additional evaporation which has the consequence of increasing low and medium cloudiness, either in surface area or in opacity power by increasing their density, which in both cases increases their cooling power. Hence, when the production of this cloudiness develops following this warming, this new or more opaque cloudiness contributes to cooling what is under it, therefore the UOS, whose heat ends up starting to decrease with a certain delay. But then, the production of cloudiness also begins to decrease since there is less evaporation, which in turn leads to further warming of the UOS since it is better exposed to solar radiation. And this cycle can be repeated. In our opinion, we are therefore dealing with an interaction that can be compared to a two-stroke engine whose pistons would be the heat of the UOS and the OC. As for the 3-month cycles for the heat present in the UOS, they come from another interaction, the one that was highlighted by Zeltz[24] with the same "signal" techniques between the heat of the UOS and global average atmospheric temperature. Cycles which had been explained in particular by the cooling of the water which undergoes evaporation, but which the present study shows that they are undoubtedly further amplified by the reciprocal influence between the UOS and the OC."

The previous Z.1 model was slightly adapted into a Z.2 model to incorporate this explanation. Specifically, line 6 of Z.1, which rudimentarily modeled atmospheric albedo, was split into lines 6a and 6b in Z.2. This modification accounted for the interaction between OC and the heat of the UOS, allowing the resulting albedo to be redefined. The remaining 16 lines of Z.1 were retained in their entirety without any further addition to form the Z.2 model.

We reproduced Figure 3 of the study[25] as Figure 4 here, illustrating the "natural thermostat" effect exerted by OC. It provides comparisons of simulations of oceanic and atmospheric temperatures generated by the Z.2 model with those produced by the Z.1 model, which did not take into account the OC parameter.

Over the period 1955 – 2095, the "natural thermostat" effect played by cloudiness was evaluated using 250 simulations, revealing a negative feedback of approximately 1°C for atmospheric temperature and approximately 2°C for UOS temperature.

Concerning MAL itself, this third study[25] exploits a very interesting property. In section 2.3 of the article, the author provides probability-based justification that, even when the processed data contain significant uncertainty (as was the case for the OC data, for which Eastman *et al.*[30] ensured an uncertainty of <5%), this uncertainty largely diminishes when it comes to the 0 or 1 signals representing quarter-to-quarter increases or decreases. This demonstrates the remarkable robustness of the signals obtained through the MAL method.

This strength of the MAL method allows it to compensate for the lack of reliability that persists in the current knowledge regarding the spatio-temporal variability of cloudiness and the dynamics of the upper mixed layer. The signal detected is clear and constructed over a sufficiently long period to warrant its consideration and investigation into the interaction it signifies. Traditional statistical methods do not provide reliable trends in such cases, which is one of the most important reasons for disparities in the quantitative assessments of future global warming rates provided by leading climate institutes.[31]

3.4. The fourth application of MAL

In this last example,[26] the author's first objective was to explain the increase in the stratification of UOS observed since 1955, notably by Li *et al.*[32] and Sallée *et al.*[33]

For this purpose, he used half-yearly UOS stratification data over the period 1955 – 2023, sourced from the same dataset used by Li *et al.*[32] (downloadable from the provided link[2]).

The application of MAL to analyze these stratification data resulted in the detection of a Markov-1 lengthening type signal. According to the author, this signal reflects the interaction with the El Niño-Southern Oscillation (ENSO), which explains its nature. Other important climatic phenomena, such as Summer-Winter Seasonal Alternation and Intertropical Convergence Zone, also play a role in the

[1] https://www.climate.gov/media/13603

[2] https://pan.cstcloud.cn/web/share.html?hash=E0zjDQOeRfs

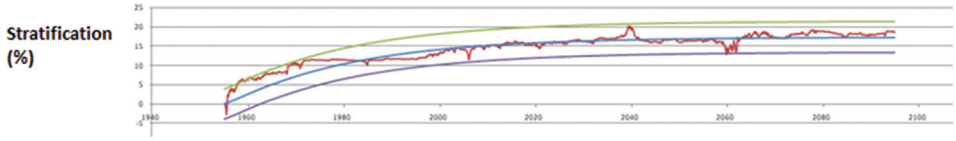

Figure 3. Simulations of Z.3 model for stratification anomalies. Reproduced from Zeltz[26]. Notes: Red curve: Simulation of anomalies of stratification, sn (%). For the other curves: The 95% confidence interval is delimited by the upper curve and lower curve. The central blue curve is the theoretical curve (without taking into account natural variability) of the stratification anomalies.

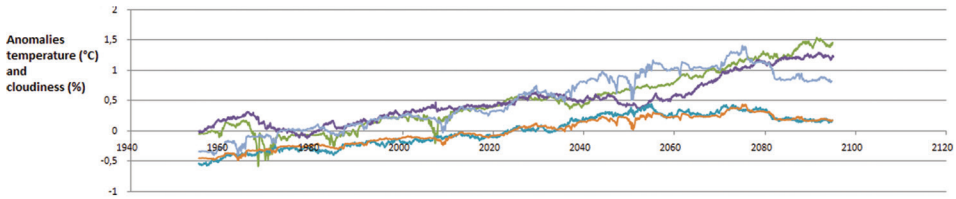

Figure 4. Graphs concerning simulations of θ_n, t_n, and cl_n for the period 1955 – 2095. Simulations of θ_n (green) and t_n (purple) anomalies (°C) were generated using the **Z.1** model. Simulations of θ_n (orange) and t_n (blue) anomalies (°C) were generated using the **Z.2** model. Simulations of cl_n (light blue)anomalies (%) were generated using the **Z.2** model (light blue curve). According to Zeltz[25]. Notes: θ_n: UOS temperature anomalies; t_n: Atmospheric temperature anomalies; cl_n: Oceanic cloudiness anomalies.

obtained signal, primarily by accelerating the half-yearly alternation. However, the dominant influence of ENSO ultimately results in a Markov-1 lengthening signal, with periodicities closely aligned with the three ENSO phases: El Niño, La Niña, and neutral events.

Once again, MAL has demonstrated its effectiveness. However, the study[26] revealed one of its limitations: the detected signal does not provide any clue to explain the observed increase in stratification within the upper 0 – 200 m ocean layer, which increased by approximately 1% per decade over the period 1955 – 2023. Moreover, there is a non-significant correlation (0.13) between the evolution of stratification and the ENSO index used.[26]

On the other hand, Zeltz[26] noted a significant correlation (0.84) between the six-monthly evolutions of this oceanic stratification and the thermal energy present in the UOS. This suggests that the increase in stratification is driven by the additional heat entering the UOS, a factor not directly identified by MAL. Summarizing the findings, the author stated: "In summary, ENSO lengthens the alternation periods, the arrival of additional heat in the UOS increases the stratification."

As this last example clearly shows, MAL can sometimes overlook very strong interactions, so users must be aware of this. That said, the MAL analysis of the stratification data successfully identified a significant interaction, which contributed to enhancing the Z.2 model by incorporating two new parameters into the global climate framework: oceanic stratification and the deepening of the mixed layer.

To help understand what may seem a paradox, Zeltz[26] uses the following metaphor:

"An analogy can help illustrate the distinction between these two types of information. Consider a musician using an electronic synthesizer: They can lengthen the cumulative duration of the ascending and descending phases of the sound power (analogous to alternation patterns) or adjust the average sound power using the potentiometer on their amplifier (analogous to quantitative variations). These are two distinct processes: the average sound power is directly influenced by the potentiometer, while the alternation speed is governed by the musician's rhythmic choices."

MAL detects the lengthening of the ascending and descending phases caused by the musician but is unable to detect the increase in power, which results from the adjustments made to the potentiometer. The Z.3 model, however, accounts for this by incorporating five of the most important parameters that define the global climate. Figures 1, 3, 5, 6 below illustrate simulations obtained from the Z.3 model (corresponding to Figures 6-9 of the last study[26]).

These graphs led the author to hypothesize a finite asymptotic growth behavior, which was mathematically proven using the relationships from the Z.3 model. The simulations produced by the model raise serious questions about some of the recent conclusions drawn by the IPCC. Specifically, while the Intergovernmental Panel on Climate Change (IPCC)[34] predicts an average global atmospheric warming of 3°C by 2100 under the same scenario, the Z.3 model forecasts a much lower increase of 1.5°C at most.

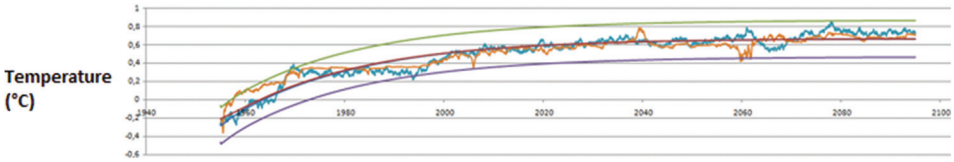

Figure 5. Simulations of Z.3 model for temperature anomalies. Reproduced from Zeltz[26]. Notes: Simulations of atmospheric temperature anomalies, tn (blue) and UOS temperature anomalies, θn (orange) anomalies (°C). For other curves: the 95% confidence interval is delimited by the upper curve and lower curve. The two central curves, which nearly overlap, are the theoretical curves (without taking into account natural variability) of tn and θn.

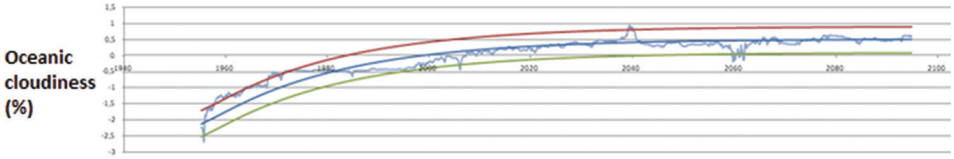

Figure 6. Simulations of Z.3 model for oceanic cloudiness anomalies. Reproduced from Zeltz[26]. Notes: Light blue curve: Simulation of anomalies of oceanic cloudiness, cln (%). For the other curves: The 95% confidence interval is delimited by the upper curve and lower curve. The central blue curve is the theoretical curve (without taking into account natural variability) of the oceanic cloudiness anomalies.

4. Evaluation and perspective of MAL

4.1. Main assets

Below is a summary of the key discoveries enabled by MAL across the four studies described in the previous section:

- Direct contributions:
  1. Interaction between the quarterly UOS heat and the monthly atmospheric temperature changes is explained by the differences in climatic memory and mediated through oceanic evaporation.
  2. Natural thermostat role played by OC on the UOS.
  3. Three-way interaction among the UOS, the OC, and the temperature of the atmosphere mediated through oceanic evaporation.
  4. The influence of ENSO on the detected signal observed in stratification data.
- Indirect contributions (through the Z.3 model):
  5. Clarity on the relationships between global warming, oceanic stratification, and the sinking of the mixed layer.
  6. Detection and mathematical demonstration of finite asymptotic growth behavior of five important climate parameters – atmospheric temperature, UOS temperature, OC, oceanic stratification, sinking of the mixed layer – in the context of current warming caused by the increase in greenhouse gases
  7. Predicting significantly lower asymptotic growth values for global warming parameters by 2100 challenging the IPCC's projections.
- Additional contributions
  8. Robustness of the generated signals, even in the event of significant uncertainties in the data series[25].
  9. The simplicity of the method – application can be performed using a simple microcomputer without any difficulty.
  10. Unlike traditional statistical methods for analyzing climatic time series, MAL results are not influenced by subjective decisions, such as the choice of the adjustment interval for estimating trends. A signal in MAL depends solely on the data series analyzed, eliminating biases introduced by arbitrary methodological choices (as highlighted by Mudelsee[6]).

In addition to the strengths already listed, some specific situations arise during the application of MAL, requiring tailored approaches to fully leverage the method's potential. The case of a Markov-0 binomial type signal (where the chains of 0 and 1 seem to be governed by a simple binomial law) is a bit special because they do not immediately impose an interaction with another climatic entity. However, this does not imply the absence of interactions – on the contrary, it is highly unlikely that any climatic parameter is entirely independent. In this case, one should search for potential interactions, prioritizing data series that exhibit similar signal characteristics.

In some instances, a signal may exhibit a "neutral" or "borderline" character, where it is neither clearly Markov-0 binomial nor distinctly Markov-1 alternating or lengthening. The following section will delve further into how changes in periodicity influence signal interpretation and how MAL can navigate these challenges effectively.

4.2. The example of stratification data

This section explores the ocean stratification data from Li *et al.*,[32] which was exploited by Zeltz.[25]

After completing the various necessary stages of the MAL (as described in Section 2.2), Table 2 summarizes the observations made on the chain lengths according to two criteria: The type of layer (0 – 2000 m or 0 – 200 m) and the period considered (month, quarter, semester, and year).

The following observations were noted:

- For the monthly data of the two layers, a mixed behavior, sometimes of Markov-1 lengthening type, other times of Markov-0 binomial type.
- For quarterly UOS data, the Markov-1 lengthening type behavior slightly prevails over the Markov-0 binomial type, though not clear.
- For the quarterly data from the upper 0 – 2000 m layer, the behavior is very pronounced Markov-1 lengthening type. Modeled by the binomial law with parameters $n = 100$ and $P = 0.5$, such a situation would be extremely improbable (less than one chance in a hundred thousand)
- For the UOS half-yearly data, the behavior is also of the very pronounced Markov-1 lengthening type. Modeled by the binomial law with parameters $n = 137$ and $P = 0.5$, such a situation would be very improbable (less than one chance in a hundred);
- For the half-yearly data from the 0 – 2000 m layer, the Markov-0 binomial type behavior takes precedence over the Markov-1 lengthening type.
- For the annual data of the two layers, the average lengths correspond well to the Markov-0 binomial case. The value of 1.92 for the ascent chains is within the required range (1.80 – 2.10). The value of 1.70 for the descent chains is certainly slightly below the lower limit of 1.80, but not significantly enough to challenge the Markov-0 binomial observation, as the 68 annual occurrences are not statistically sufficient for a tightly defined range with high confidence. It is more likely that this exceptional value, compared to all others, results from potential strong fluctuations in the average of a small sample.

Asking the following four questions, therefore, becomes imperative:

- Question 1: How can the rather Markov-1 lengthening type behavior for the half-yearly UOS stratification data be explained?
- Question 2: Why do the annual changes in the stratifications of the two layers exhibit a Markov-0 binomial-type behavior, appearing to lose all "memory" of the previous year from 1 year to the next?
- Question 3: Why are the quarterly stratification data of the upper 0 – 2000 m layer clearly of the Markov-1 lengthening type, while this is less evident for the UOS? And why is the opposite observed for the half-

Table 2. Average chain lengths of 1s and 0s for the 0 – 2000 m or 0 – 200 m (UOS) layers by month, quarter, semester, and year

Monthly	**Layers**	**0 – 2000 m**		**0 – 200 m (UOS)**	
	Chains of	**1**	**0**	**1**	**0**
1955 – 2023	Average	2.20	2.05	2.20	2.08
Total:827 values	Nb. of chains	270	257	268	262
1955 – 1965	Average	2.31	1.95	2.33	1.93
Total: 127 values	Nb. of chains	42	44	42	45
1965 – 1974	Average	2.82	2.13	2.54	1.88
Total: 100 values	Nb. of chains	34	30	35	33
1974 – 1982	Average	2.72	1.81	2.06	1.94
Total: 100 values	Nb. of chains	32	26	31	33
1982 – 1990	Average	2.06	1.97	2.75	1.96
Total: 100 values	Nb. of chains	32	34	32	26
1990 – 1999	Average	1.94	1.97	2.08	1.94
Total: 100 values	Nb. of chains	34	34	34	33
1999 – 2007	Average	2.00	1.90	1.88	2
Total: 100 valeurs	Nb. of chains	34	32	34	33
2007 – 2016	Average	1.88	2.06	1.9	2.10
Total: 100 values	Nb. of chains	32	31	32	31
2016 – 2023	Average	2.42	2.06	2.65	2.19
Total: 100 values	Nb. of chains	26	31	26	26
Quarterly	**Layers**	**0–2000 m**		**0–200 m (UOS)**	
	Chains of	**1**	**0**	**1**	**0**
1955 – 2023	Average	2. 35	2.35	2.13	2.04
Total: 275 values	Nb. of chains	80	70	84	79
1955 – 1978	Average	2.38	2.25	2.28	2.36
Total: 90 values	Nb. of chains	26	20	26	24
1978 – 2000	Average	2.66	2.63	2.21	1.93
Total: 90 values	Nb. of chains	27	16	30	26
2000 – 2023	Average	2.45	2.04	2.20	1.89
Total: 95 values	Nb. of chains	33	25	31	26
Semesterly	**Layers**	**0 – 2000 m**		**0 – 200 m (UOS)**	
	Chains of	**1**	**0**	**1**	**0**
1955 – 2023	Average	2.2	2.00	2.74	2.37
Total: 137 values	Nb. of chains	45	38	27	27
Yearly	**Layers**	**0 – 2000 m**		**0 – 200 m (UOS)**	
	Chains of	**1**	**0**	**1**	**0**
1955 – 2023	Average	1.92	1.70	1.92	1.7
Total: 68 values	Nb. of chains	24	20	24	20

yearly data?

- Question 4: Why do the monthly evolutions of the two layers oscillate between a Markov-0 binomial type and a faintly Markov-1 lengthening type?

The answer to Question 1 is provided in detail in section 3.1 of Zeltz,[26] reproduced in full in Appendix File. In summary:

As indicated by Sallée *et al.*,[33] a seasonal summer-winter alternation exists, particularly in temperate and cold zones, where a seasonal thermocline forms in summer (reinforced by the ice melting[35] and weakens in winter[36]). Likewise, the Intertropical Convergence Zone (ITCZ) contributes to a biannual alternation.[37] If only these two were at play, a biannual Markov-1 alternating signal would emerge. However, as demonstrated by Zeltz,[26] particularly through the index studied by Trenberth[38] the dominant influence of ENSO with its El Niño and La Niña phenomena, which explains that the Markov 1 lengthening type signal.

For Question 2, we propose the following explanation:

Unlike the semesters, over an entire year, the impacts of the ITCZ and the stratification caused by summer heat in the two hemispheres are balanced and neutralized. As for the "lengthening" impact, the average duration of the events involved (9 months for El Niño and La Niña, and 6 months for a neutral period), is too short to significantly increase the probability of repetition in the following year. Therefore, the annual fluctuations in the stratification of the UOS and the 0 – 2000 m layer exhibit a Markov-0 binomial-type behavior.

For Question 3, we propose the following explanation:

For the upper 0 – 2000 m layer, the quarterly stratification data strongly exhibit a Markov-1 lengthening type behavior, whereas this is not as pronounced for the UOS layer. To clarify, this does not mean that stratification increases more strongly on a quarterly basis in the 0 – 2000 m layer; rather, it means that if stratification increases (or decreases) in one quarter, the probability that it will continue to increase (or decrease) in the next quarter is higher than vice versa.

The explanation for this pattern is still largely linked to the ENSO phenomenon and this is how:

At the core of El Niño and La Niña events, there is a disruption of the trade winds compared to their ordinary regime. During an El Niño event, these winds weaken significantly due to an abnormally weak anticyclone, a phenomenon linked to the Walker convective loop but not yet fully understood.[39-42] This disruption has repercussions on the circulation of the equatorial underlying current (EUC)[43] which usually flows in the same area. The EUC, a significant and cold current equivalent to the flow of about 150 Amazon Rivers, has its core along the thermocline and generally moves eastward due to the stress exerted by westward-flowing trade winds. This creates a stratified shear flow, giving the main thermocline its characteristic slope.[44] However, when the trade winds weaken, the slope of the main thermocline is modified, causing the EUC to change direction. This, in turn, modifies the stratification of the upper 0 – 2000 m layer, which contains the thermocline located below the UOS. Given the scale of the phenomenon, its impact is readily observed in the global average stratification of the layer. Moreover, this effect manifests more quickly than temperature changes induced by El Niño-related water movement, which take longer to develop due to the thermal inertia involved.

Hence, shortly after the establishment of this new regimen, changes in stratification are felt in the 0 – 2000 m layer, becoming clearly visible during the current quarter and likely persisting into the following quarter. This explains the strongly "lengthening" character of the quarterly stratification signal for this layer. However, as the El Niño event reaches its full strength, stratification changes in this layer gradually return to standard behavior, causing the signal to quickly lose its "lengthening" characteristic at the half-year level for the upper 0 – 2000 m layer. Conversely, the UOS layer begins to be progressively affected by temperature changes that modify its stratification, eventually displaying a more pronounced "lengthening" characteristic at the half-year level. This described behavior of the EUC is certainly not a unique case; similar phenomena, such as those observed in the Weddel Sea under the influence of ENSO, further corroborate this pattern.[45]

For La Niña, unlike El Niño, deep convection is reinforced in the west of the basin while the trade winds gain intensity. Therefore, the inclination of the thermocline further increases compared to normal conditions, which strengthens the EUC in the eastward direction.[38] This results in cold temperature anomalies in the eastern Pacific and warm surface waters near the Asian coasts. These changes occur with a similar lag as in El Niño events, where the purely dynamic and mechanical modifications to stratification at the thermocline appear relatively quickly, while those of thermal origin take longer to manifest in the UOS.

And finally here is our answer to the Question 4:

Whether dynamic or thermal in nature, the effects on stratification of events such as El Niño or La Niña may not be sufficiently established to appear clearly in stratification signals during the 1st month following their onset in the Pacific zone. Furthermore, over the 100 consecutive months considered, there are long sub-periods without

the occurrence of these events. This likely explains why, for both layers, we observe a fairly balanced mix of monthly Markov-0 binomial type signals and Markov-1 lengthening type signals.

Thus, the fact that the signal may vary depending on the period considered (month, quarter, half-year, year) not only avoids real contradictions but also is well-explained and, in fact, contributes to a better understanding of the mechanisms at play.

4.3. The main reason for the effectiveness of MAL

The effectiveness of MAL lies primarily in its comparison of two "spectra"—the spectra of 0 and 1 for each of the two series being analyzed. Unlike other techniques, which rely on raw initial data or, in some cases, derived data (e.g., differences of successive terms for deseasonalization), MAL focuses solely on the binary aspect of whether the data increase or decrease. This transition from raw data to their "spectrum" leads to a huge loss of information, retaining only this critical piece: the direction of change. However, by isolating this single piece of information, MAL prevents it from being overshadowed by other elements in the raw data, enabling it to detect signals and interactions that other statistical techniques do not detect.

4.4. Possible use of MAL in sectors other than climatology

Time series have long concerned many sectors other than climatology, including econometrics, information theory, demography, astronomy, and epidemiology.[2-5,46-49]

Similar to its application in climatology, MAL can be effective in other fields, provided the digital data studied meet the necessary conditions for MAL processing, particularly that their successive deviations have the same probability of being positive or negative. Additionally, the field must be complex enough to exhibit multiple and varied interactions, a scenario where the method is well-suited for identifying potential interactions, as demonstrated in climatology. However, these conditions are restrictive, and only practical experiments can determine whether MAL proves valuable outside climatology.

It is worth noting that the concept of using Markov chains to analyze time series data is not new; for instance, it was employed as early as 1966 by Lortet-Zuckermann[3] to analyze a series of 444 successive explosions of the star SS Cygni observed from 1896 to 1957.

5. Conclusion

MAL is a new method for analyzing climatic time series based on the length of rise or fall chains in the studied climatic data. When fully implemented, the signals obtained provide valuable information, enabling precise identification of the mechanisms and interactions at play.

While this method does not reveal everything or decode all the climatic parameters at stake, MAL undoubtedly serves as a valuable additional tool for enhancing our understanding of the climate and achieving more reliable long-term projections.

The examples described in this clearly demonstrate the value of the method, yielding results of significant importance in climatology, such as:

- Detecting and explaining a phenomenon of "natural nervousness," where global average temperature differences have a greater tendency to reverse their sign than maintain it from 1 month to the next.[24]
- Demonstrating, in what seems a definitive way, that cloudiness provides clearly negative feedback on global warming, with the OC acting as a natural thermostat of the climate.[25]
- Establishing that the parameters most critical to defining the global climate exhibit limited long-term growth, predicting temperature increases by 2100 significantly lower than current IPCC projections.[26]

Moreover, nothing a priori prevents MAL from being applied in other sectors beyond climatology, as long as the system is complex and time series data are available.

Acknowledgments

None.

Funding

None.

Conflict of interest

The author declares no conflicts of interest.

Author contributions

This is a single-authored article.

Ethics approval and consent to participate

Not applicable.

Consent for publication

Not applicable.

Availability of data

Data are available from the corresponding author upon reasonable request.

References

1. Hamilton JD. *Time Series Analysis*. Princeton, USA: Princeton University Press; 1994. p. XIV+799.
2. Ash RB. *Information Theory*. New York, USA: Wiley Inter Science; 1965. p. XI+345.
3. Lortet-Zuckermann MC. Testing the Chain Hypothesis of Markov. Application to the succession of various kinds. Explorations of SS Cyg. *Ann Astrophys*. 1966;29:205-222.
4. Amegandjin J. *Démographie Mathématique*. Paris: Economica; 1989. p. 265.
5. Bourbonnais R, Terraza M. Éco Sup. In: *Analyse des Séries Temporelles: Applications à l'économie et à la Gestion*. 4th ed. Paris: Dunod; 2016. p. 368.
6. Mudelsee M. Trend analysis of climate time series: A review of methods. *Earth Sci Rev.* 2019;190:310-322.

   doi: 10.1016/j.earscirev.2018.12.005
7. Brockwell PJ, Davis RA. *Time Series: Theory and Methods*. 2nd ed. New York: Springer; 1991. p. 577.
8. Montgomery DC, Peck EA. *Introduction to Linear Regression Analysis*. 2nd ed. New York: Wiley; 1992. p. 527.
9. Sen A, Srivastava M. *Regression Analysis: Theory, Methods, and Applications.* New York: Springer; 1990. p. 347.
10. Mudelsee M. Ramp function regression: A tool for quantifying climate transitions *Comput Geosci*. 2000;26(3):293-307.

    doi: 10.1016/S0098-3004(99)00141-7
11. Lahiri SN. *Resampling Methods for Dependent Data*. New York: Springer; 2003. p. 374 .
12. Doukhan P, Oppenheim G, Taqqu MS. *Theory and Applications of Long-Range Dependence*. Boston: Birkhäuser; 2003. p. 719.
13. Hall P. Theoretical comparison of bootstrap confidence intervals. *Ann Stat*. 1988;16(3):927-985.

    doi: 10.1214/aos/1176350933
14. Efron B. Bootstrap methods: Another look at the jackknife. *Ann Stat*. 1979;7(1):1-26.

    doi: 10.1214/aos/1176344552
15. Gallant AR. *Nonlinear Statistical Models*. New York: Wiley; 1987. p. 610.
16. Seber GAF, Wild CJ. *Nonlinear Regression*. New York: Wiley; 1989. p. 768.
17. Granger CWJ, Newbold P. Spurious regressions in econometrics. *J Econom*. 1974;2:111-120.

    doi: 10.1016/0304-4076(74)90034-7
18. Engle RF, Granger CWJ. Co-integration and error correction*: Representation,* estimation and testing. *Econometrica*. 1987;55:251-276.

    doi: 10.2307/1913236
19. Johansen S. Estimation and hypothesis testing of cointegration vectors in gaussian vector autoregressive models. *Econometrica*. 1991;59:1551-1580.

    doi: 10.2307/2938278
20. Stock JH, Watson MW. A Simple estimator of cointegrating vectors in higher order integrated systems. *Econometrica*. 1993;61:783-820.

    doi: 10.2307/2951763
21. Phillips PCB, Ouliaris S. Asymptotic properties of residual based tests for cointegration. *Econometrica.* 1990;58:165-193.

    doi: 10.2307/2938339
22. Granger CWJ. Some recent development in a concept of causality. *J Econom*. 1988;39:199-211.

    doi: 10.1016/0304-4076(88)90045-0
23. Zeltz É. Analysis and climatological interpretation of the evolution of global mean temperatures since 1880. *Physio-Géo*. 2021;16(1):49-70.

    doi: 10.4000/physio-geo.12176
24. Zeltz É. Origins of "natural climatic nervousness" and its current accentuation. *J Mod Green Energy*. 2023;2:8.

    doi: 10.53964/jmge.2023008
25. Zeltz É. Analysis of the interaction of oceanic cloudiness with the upper oceanic stratum. *J Inform Anal*. 2024;2:4.

    doi: 10.53964/jia.2024004
26. Zeltz É. Mechanisms driving ocean stratification and mixed layer deepening. *Explora Environ Resour*. 2024;1(1):4578.

    doi: 10.36922/eer.4578
27. Delmas JF. *Stochastic Processes and Applications*. Available from: https://cermics.enpc.fr/~delmas/Enseig/proba2-notes.pdf [Last accessed on 2025 Feb 03].
28. Taboada JJ. *Cosmic Rays: Influences on Climate and Eteorology.* SlideShare; 2010. Available from: https://fr.slideshare.net/slideshow/jj-taboada-c-rays-climate/3171290 [Last accessed on 2024 Dec 20].
29. Hasselmann K. Stochastic climate models: Part I. Theory. *Tellus*. 1976;28:473-485.

    doi: 10.3402/tellusa.v28i6.11316
30. Eastman R, Warren SG, Hahn CJ. Variations in cloud cover and cloud types over the ocean from surface observations, 1954-2008. *J Clim*. 2011;24:5914-5934.

    doi: 10.1175/2011JCLI3972.1
31. World Climate Research Programme. *WCRP Grand Challenge on Clouds, Circulation and Climate Sensitivity*. Available from: https://www.wcrp-climate.org/gc-clouds [Last accessed on 2024 Dec 20].

32. Li G, Cheng L, Zhu J, Trenberth KE, Mann ME, Abraham JP. Increasing ocean stratification over the past half-century. *Nat Clim Chang*. 2020;10:1116-1123.

doi: 10.1038/s41558-020-00918-2

33. Sallée JB, Pellichero V, Akhoudas C, *et al*. Summertime increases in upper-ocean stratification and mixed-layer depth. *Nature*. 2021;591:592-598.

doi: 10.1038/s41586-021-03303-x

34. Intergovernmental Panel on Climate Change. Sea level rise and implications for low-lying Islands, coasts and communities. In: *Special Report on the Ocean and Cryosphere in a Changing Climate*. Ch. 4., Table. 4.1. Geneva, Switzerland: Intergovernmental Panel on Climate Change; 2019. p. 336.

35. Lacombe H. *Généralités sur les Thermoclines, Leur Genèse et Leur Prévision. Exposé Introductif*. La Houille Blanche/N 7/8-1974; 1974.

36. Haine TWN, Curry B, Gerdes R, *et al*. Arctic freshwater export: Status, mechanisms, and prospects. *Glob Planet Change*. 2015;125:13-35.

doi: 10.1016/j.gloplacha.2014.11.013

37. Schneider T, Bischoff T, Haug GH. Migrations and dynamics of the intertropical convergence zone. *Nature*. 2014;513(7516):45-53.

doi: 10.1038/nature13636

38. Trenberth K, National Center for Atmospheric Research Staff, editors. *The Climate Data Guide: Nino SST Indices* (*Nino 1+2, 3, 3.4, 4; ONI and TNI*). Climate Data Guide; 2023.

39. *Météo Contact "Partageons le Temps de Demain*. Available from: https://www.meteocontact.fr/pour-aller-plus-loin/el-nino-la-nina#google_vignette [Last accessed on 2024 Dec 20].

40. Abarca Del Rio A, Gambis D, Salstein D, Dewitte B. El Niño et la rotation de la terre. *Pour Sci*. 2001;281:78-82.

41. Clarke AJ. *An Introduction to the Dynamics of El Niño and the Southern Oscillation*. United States: Academic Press; 2008. p. 308.

42. Sarachik ES, Cane MA. *The El Niño-Southern Oscillation Phenomenon*. Cambridge: Cambridge University Press; 2010. p. 369.

43. Cromwell T, Montgomery RB, Stroup ED. Equatorial undercurrent in Pacific Ocean revealed by new methods. *Science*. 1954;119(3097):648-649.

doi: 10.1126/science.119.3097.648

44. Strang EJ, Fernando HJS. Vertical mixing and transports through a stratified shear layer. *J Phys Oceanogr*. 2001;31:2026-2048.

doi: 10.1175/1520-0485(2001)031<2026:VMATTA>2.0.CO;2

45. Gordon AL, Huber B, McKee D, Visbeck M. A seasonal cycle in the export of bottom water from the Weddell Sea. *Nat Geosci*. 2010;3:551-556.

doi: 10.1038/ngeo916

46. Box G, Jenkins G. *Time Series Analysis: Forecasting and Control*. Deerfield, IL: Holden-Day; 1970.

47. Bresson G, Pirotte A. *Économétrie des Séries Temporelles: Théorie et Applications*. Paris: Presses Universitaires de France; 1995.

48. Vandenhouten R. *Non-stationary Time Series Analysis of Complex Systems and Applications in Physiology*. Aachen: Shaker Verlag GmbH; 1998.

49. Pirotte A. *L'économétrie: Des Origines aux Développements Récents*. Paris: CNRS; 2004. p. 242.

Appendix

Table A1 summarizes the average lengths of strings of 0 and 1 per semester for the UOS.

We notice the behavior of the very pronounced Markov-1 lengthening type. Modeled by the binomial law with parameters $n = 137$ and $P = 0.5$, such a situation would be very improbable (<1 chance in a hundred).

How to explain the rather Markov-1 lengthening type behavior for the half-yearly UOS stratification data?

Here is our detailed response to this question:

Sallée *et al.*[1] clearly indicate the summer-winter seasonal alternation which concerns the stratification of the UOS. Notably because in temperate and cold zones, there is in the 0 –200 m layer the presence of a seasonal thermocline in summer reinforced in particular by the melting of the ice[2] and which breaks down in winter.[3] Note that summer (winter) refers to August-October in the northern (southern) hemisphere and January-March in the southern (northern) hemisphere. Moreover, the significant imbalance in the land-sea relationship between the two hemispheres (80% of the surface area of the southern hemisphere is marine compared to only 60% of the northern hemisphere) means that there is no full compensation of the average stratification of that of the south by that of the north. Hence, if it was only this aspect that intervened, we should observe a half-yearly signal of the Markov-1 alternating type. However, it is of the Markov-1 lengthening type.

So necessarily, other phenomena intervene in the opposite direction. That of the influence of the Intertropical Convergence Zone (ITCZ) is undoubtedly one of them:

The ITCZ is more in the Southern Hemisphere during the austral summer and more in the Northern Hemisphere during the boreal summer.

However, the ITCZ brings rainy seasons and monsoons which cool the UOS in the vast ocean areas concerned and therefore reduce the stratification resulting from warming. The marine coverage of the ITCZ is much greater when it is positioned south of the Equator than in the north and therefore counterbalances the stratification caused by the austral summer on the temperate latitudes of this hemisphere. Likewise on the other hemisphere with related proportions. This phenomenon therefore certainly compensates for a large part of the summer increase in stratification present in the temperate zones of the hemisphere where the ITCZ is temporarily positioned. If there were no other influences, the signal would be of binomial Markov-0 type or close to it. However, it is clearly of the Markov-1 lengthening type. Hence, there is still at least one important additional influence which intervenes in the half-yearly evolution of the stratification of the UOS.

Table A1. Average lengths of chains of 1s and 0s following the 0 – 200 m (UOS) layer per semester

Per semester	Layers:	0 à 200m (UOS)	
Periods	Chains of:	1	0
Total (1955 – 2023)	Average:	2.74	2.37
137 values 0 or 1	Nb. of chains:	27	27

As we show below, using the statistics for El Niño and La Niña events obtained with the ONI index indicates that the "lengthening" character of the semiannual signal certainly comes largely from this influence. The ONI index used is an index provided by NOAA and downloadable from the following link: https://origin.cpc.ncep.noaa.gov/products/analysis_monitoring/ensostuff/ONI_v5.php

The drastic rules applied to it to obtain it and the large geographical area over which it is calculated (5N-5S, 170W-120W) make it, in our opinion, the El Niño-Southern Oscillation (ENSO) index best suited for our study among those that exist (cf. Trenberth[4]).

According to him, over the 74 years of the period 1950 – 2023, the cumulative equivalent of approximately 21 years was affected by El Niño, that of approximately 22 years by La Niña and that of approximately 33 years is "normal," that is to say neither affected by El Niño nor affected by La Niña. Still according to this index, the average duration is about 9 months (more precisely 8.65) per El Niño event, about 9 months (9.21) per La Niña event and about 6 months (6.03) per neutral event. So if for example during a semester the stratification rises following an El Niño event, there is a greater probability that the following quarter it will continue to rise, since the El Niño event with an average duration of 9 months is very likely to last at least a few more months for the next semester. Likewise, if for one semester the stratification decreases following a La Niña event of average duration 9 months, there is a greater probability that it will continue to decrease the following semester, rather than it increase. Given the high frequency of such events (together, they cover 58.5% of the entire period 1950 – 2023), this is largely sufficient to explain the fact that the biannual chains concerning the stratification of the UOS and layer 0 – 2000 m above are pronounced Markov 1 lengthening type.

References

1. Sallée JB, Pellichero V, Akhoudas C, *et al.* Summertime increases in upper-ocean stratification and mixed-layer depth. *Nature*. 2021;591:592-598.

doi: 10.1038/s41586-021-03303-x

2. Lacombe H. *Généralités sur les Thermoclines, Leur Genèse et leur Prévision. Exposé Introductif*. La Houille/N 7/8-1974; 1974.

3. Haine TWN, Curry B, Gerdes R, *et al*. Arctic freshwater export: Status, mechanisms, and prospects. *Glob Planet Change*. 2015;125:13-35.

doi: 10.1016/j.gloplacha.2014.11.013

4. Trenberth K, National Center for Atmospheric Research Staff, editors. *The Climate Data Guide: Nino SST Indices* (*Nino 1+2, 3, 3.4, 4; ONI and TNI*); 2024. Available from: https://climatedataguide.ucar.edu/climate-data/nino-sst-indicesnino-12-3-34-4-oni-and-tni%20on%20%5b%20last%20accessed%20on%202024-12-02"https://climatedataguide.ucar.edu/climate-data/nino-sst-indices-nino-12-3-34-4-oni-and-tni on [Last accessed on 2024 Dec 02].